Astron. Astrophys. 237, 3–11 (1990)

ASTRONOMY AND ASTROPHYSICS

43 GHz-VLBI observations of 3C 273 after a flux density outburst in 1988

T.P. Krichbaum[1], R.S. Booth,[2] A.J. Kus[2], B.O. Rönnäng[2], A. Witzel[1], D.A. Graham[1], I.I.K. Pauliny-Toth[1], A. Quirrenbach[1], C.A. Hummel[1], A. Alberdi[1,11], J.A. Zensus[3,6], K.J. Johnston[4], J.H, Spencer[4], A.E.E. Rogers[5], C.R. Lawrence[6], A.C.S. Readhead[6], H. Hirabayashi[7,8], M. Inoue[7], M. Morimoto[7], V. Dhawan[9,12], N. Bartel[9], I.I. Shapiro[9], B.F. Burke[10], and J.M. Marcaide[11]

[1] Max-Planck-Institut für Radioastronomie, Auf dem Hügel 69, D-5300 Bonn, Federal Republic of Germany
[2] Onsala Space Observatory, S-43900 Onsala, Sweden
[3] National Radio Astronomy Observatory, Socorro, NM 87801, USA
[4] Naval Research Laboratory, Washington, DC 20375, USA
[5] NEROC, Haystack Observatory, Westford, MA 01886, USA
[6] California Institute of Technology, Pasadena, CA 91125, USA
[7] Nobeyama Radio Observatory, Nobeyama, Nagano, 384-13, Japan
[8] Institute of Space and Astronatical Science, Tokyo, Kanagawa, 229, Japan
[9] Harvard Smithsonian Center of Astrophysics, Cambridge, MA 02139, USA
[10] Massachusetts Institute of Technology, Cambridge, MA 02139, USA
[11] Instituto de Astrofisica de Andalucia, E-18080 Granada, Spain
[12] Raman Research Institute, 560012 Bangalore, India

Received December 27, 1989; accepted March 7, 1990

Abstract. From 2 epochs of VLBI observations, we present the first 43 GHz maps of 3C 273 with an east-west resolution of 0.1 mas corresponding to 0.18 pc ($H_0 = 100\,\mathrm{km\,s^{-1}\,Mpc^{-1}}$ and $q_0 = 0.5$). After an optical/infrared flux density outburst in March 1988, also observed in the mm-region, a new component appeared close to the core (at a radial distance $r = 0.2$ mas). Reobservation of 3C 273 after 9 months revealed a more complex core-jet structure indicating superluminal expansion with apparent speed $\beta_{\mathrm{app}} = 5.5 \pm 0.8$. The ejecta appear at position angles relative to the core different from those of older components, seen at larger distances, suggesting motion along curved trajectories. The combination with data from the literature suggests a quasi-sinusoidally curved ridgeline of the jet near the core. We further identify a superluminally moving component at $r \simeq 3$ mas with a feature previously denoted C 8. Its observed path coincides, within the measurement errors, with the curved trajectory of the earlier component C 7, visible at frequencies below 43 GHz. A possible explanation of the jet oscillations is an intrinsic three-dimensional (helical) bending of the trajectories of the jet components.

Key words: interferometry – 7mm-VLBI – quasars: 3C 273 – relativistic jet physics – radio variability

1. Introduction

A primary goal of mm-VLBI observations is the investigation of the generation and evolution of powerful radio jets of active galactic nuclei (AGN) in regions very close to the "central engine". The bright quasar 3C 273 ($m_v = 13$, $z = 0.158$) exhibits violent activity and is a well-known superluminal source. The high degree of activity from the radio to the X-ray band in combination with the relative proximity of the source favour its investigation with mm-VLBI. It is now possible for the first time to investigate the unresolved and (at cm wavelength) compact center of activity (the core) and the jet emerging from it with a spatial resolution of 0.18 pc (adopting $H_0 = 100\,\mathrm{km\,s^{-1}\,Mpc^{-1}}$ and $q_0 = 0.5$), corresponding to a beamsize of 0.1 mas which we obtain with current VLBI at 43 GHz. This allows the investigation of the motion of jet components and the determination of their trajectories in regions very close to the core. Thus, direct images become available from regions otherwise accessible only by indirect methods.

At frequencies below 5 GHz, VLBI images of 3C 273 show a 50 mas long, slightly curved jet with a complex brightness distribution. There are indications that the motion of some superluminal components in this jet follow a common fixed, curved trajectory (Cohen et al., 1987, hereafter Co87; Zensus et al., 1988, hereafter Z88, Zensus et al., 1990a, hereafter Z90). Millimeter-VLBI with its higher resolution allows us to trace this bending even closer to the core.

In 1985, Marcaide et al. first detected transatlantic fringes with VLBI at 43 GHz on several bright sources, including 3C 273. In 1986, the source was again observed during an experiment primarily aimed at imaging 3C 84 (Dhawan, 1987; Bartel et al., 1988). Owing to the sparseness of the data obtained for 3C 273 and the technical problems arising at mm-wavelengths, these experiments yielded only crude estimates of the source structure.

In this paper, we present 43 GHz images of 3C 273 at epochs 1988.48 and 1989.19, obtained from VLBI-observations made shortly after a large flux density outburst in the optical/infrared

Send offprint requests to: T.P. Krichbaum

band in March 1988 (Courvoisier et al., 1988). These are the first VLBI images of 3C 273 at this frequency and they show that rapid structural changes occurred after this outburst.

2. The experiments

The observations of 3C 273 were performed on June 25, 1988 as part of a scheduled 7mm-VLBI experiment, and in an ad hoc experiment on March 8–9, 1989. The primary aim of the first experiment was the imaging of 3C 84 and 3C 345 with the best possible uv-coverage. 3C 273 was scheduled in gaps between the observation of 3C 84 and 3C 345, at times that coincided with its best common visibility by both European and American telescopes. Because of the lack of common visibility, the antenna at Nobeyama (Japan) was not scheduled to observe 3C 273. Thus, the source was observed with a 4 station sub-network [Bonn (B), Onsala (T), Haystack (K), Maryland Point (N)] starting on June 25 at 18^h00 UT for 4 hours and earlier that day on the K-N baseline for 4 hours, starting at 0^h00 UT. The good results of the first experiment led to the second, ad hoc observation of 3C 273. In this VLBI experiment, the source was observed with the best possible uv-coverage in order to check the previous results and to look for structural variability. Five stations [B, T, K, Owens Valley (O) and Nobeyama (X)] observed 3C 273 from March 8, 20^h30 UT until March 9, 14^h15 UT. In addition, the source 1803 + 78 (e.g., Schalinski et al., 1987) was observed as a calibrator before, during, and after the observations of 3C 273. The experimental setup and the characteristics of the 7-mm VLBI network are described by Krichbaum, 1990b, and also by Zensus et al., 1990b.

3. Data reduction and analysis

VLBI observations at 43 GHz can still be regarded as pioneering work. Changing weather conditions, short integration times, sparse uv-coverage, and technical difficulties with receivers and telescopes make such observations far from routine. We therefore elaborate here on the data reduction and analysis.

The data were recorded using the MkIII VLBI system (Rogers et al., 1983) with a bandwidth of 56 MHz (mode A). Each scan had a duration of 13 min. The observations were made at a center frequency of 43 222.99 MHz with left circular-polarized feeds. The data were correlated, fringe fitted, and analyzed at the Mk III correlator of the MPIfR in Bonn (for a description of the standard data reduction see, e.g., Alef, 1988a). Since 3C 273 was unusually bright ($S_{43\,\mathrm{GHz}} = 28.6$ Jy) and compact during the first experiment, we could detect strong fringes on each baseline independently with signal-to-noise ratios (SNR) up to 462 on the short baselines and not less than 8 on any baseline.

As a test, we additionally recorded the data with the smaller bandwidth of 2 MHz, using the MkII VLBI system (Clark, 1973). Not unexpectedly, some sensitive baselines (BT, BK, TK, and KN) also showed good MkII fringes.

Short timescale ($t \simeq 2$ s) phase fluctuations of the 5 MHz reference signal from the hydrogen maser at Onsala (T) during the second experiment (1989.19), resulted in coherence losses on all baselines to this station, and a station-phase correction for Onsala was necessary. Since at 43 GHz the structure visibility phase from a source with several milliarcseconds extent is much smaller than the phase noise introduced by the atmosphere, we used the 2-second visibility phases on the short, sensitive baseline B-T (where the fringes were always sufficiently strong despite the loss of coherence) as a measure of the Onsala-maser phase fluctuations and corrected the visibility phases of the remaining baselines involving T, thus recovering most detections (Krichbaum, 1990b). We note that this phase correction is station-dependent and therefore does not affect the closure-phases and the source structure. Station-dependent phase corrections cause only a shift of the visibility phases including T, but in the closure triangles this shift cancels.

The data were then segmented into 200 s intervals. For each of these segments, closure relations for fringe rate, single-band delay, and multi-band delay were computed. The data were then global-fringe-fitted following the method of Alef and Porcas (1986), which considerably improved the data quality and lowered the detection threshold. For the experiment of 1989 global-fringe-fitting resulted in detections on all baselines with SNR ≥ 5, with the exception of three low-elevation scans on the baselines B-O and T-O which had SNR ≤ 4. Due to their low SNR the latter scans were not accepted as detections and were consequently not used in the imaging process. After fringe fitting, the Mk III-data were segmented into time intervals corresponding to the length of the coherence time, i.e. 26 s (13 times the pre-integration time of the correlator of 2 s). This was found to lead to amplitude losses below 10% for all baselines, although for some scans the coherence time was much longer.

At mm-wavelengths the atmosphere strongly influences the measurements, and therefore special care was taken in the amplitude calibration of the VLBI data. Before and during the VLBI experiments we determined the flux density scale with the 100m-telescope in Effelsberg by reference to the planets (Mars, Venus, Jupiter, and Saturn). Before and after each 13 min VLBI scan, the system temperature T_{sys} was measured at all telescopes. Antenna temperature measurements and pointing scans in gaps between two adjacent VLBI scans were used to derive time- and elevation-dependent gain corrections. At some stations (B, T, and X) the optical depth of the atmosphere was determined from T_{sys} measurements as a function of elevation ("sky dips"). With this information the elevation-dependent atmospheric absorption was incorporated into the calibration.

The 26-second data were edited and hybrid maps were made in the usual way, using the MPIfR-Hybrid Mapping Package (e.g., Alef et al., 1988b; Witzel et al., 1988, and references therein). Additionally, the data were exported into the Caltech VLBI-Package, where they were incoherently averaged for 160 s and Gaussian components were fitted to the data (model fitting). CLEAN- and Maximum-Entropy maps were made with the averaged data (in the Caltech-package), which gave similar results to the previously derived maps from the unaveraged data. To check the calibration, we compared the station-dependent effective gain factors to those derived from maps and models of 3C 84, 3C 345, and 1803 + 78 at the same epochs (see e.g. Krichbaum, 1990c). On the basis of this comparison and the inspection of the closure amplitudes of 3C 273, we found no severe calibration errors (> 20%) for any of the sets of data. Since the amplitude calibration for Maryland Point (N) for the first epoch observations was more uncertain than for B, T, and K, we also made maps and models while allowing the gain of N to vary (time-dependent amplitude self-calibration). Because three closure amplitudes were available in 1988.48, gain corrections for N could be derived and applied to the data. The source structure derived from data self-calibrated in this way does not differ signif-

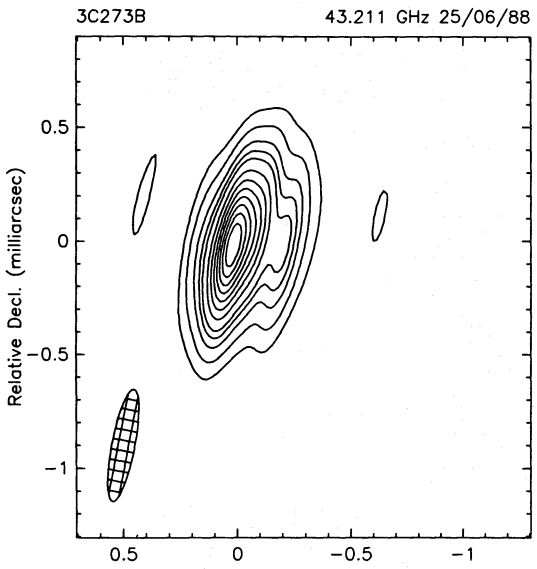

Fig. 1a. 43 GHz CLEAN-map of 3C 273, epoch 1988.48. Contours are 2, 5, 10, 15, 20, 30, 40, 50, 60, 70, 80, and 90% of the peak flux density (10.3 Jy beam^{-1}). The restoring beam is 0.5 × 0.1 mas, P.A. = −11°. The NS elongation of the beam is artificially reduced by a factor of 3

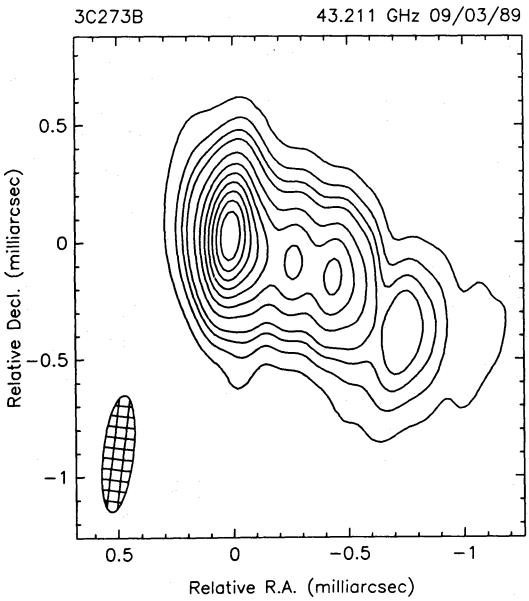

Fig. 1b. 43 GHz CLEAN-map of 3C 273, epoch 1989.19. Contours are 5, 10, 15, 20, 30, 40, 50, 60, 70, 80, and 90% of the peak flux density (5.2 Jy beam^{-1}). The restoring beam is 0.5 × 0.13 mas, P.A. = −7°. The NS elongation of the beam is artificially reduced by a factor of 2

icantly from the previously derived structure, but sidelobes and noise in the maps are reduced. Since 3C 273 has a declination of $\delta = +2°$, observations with the current 7mm VLBI network result in an elongated beam for this source, which gives high resolution in the east-west direction ($\simeq$ 0.1 mas) but low resolution in the north-south direction ($\simeq$ 1.5 mas in 1988.48 and $\simeq$ 1.0 mas in 1989.19). For a representation of the source structure more pleasing to the eye, we show in Fig. 1a and b the CLEAN-maps restored with a beam artificially reduced in NS elongation. We decided to limit the size of our maps to a field of view which is appropriate to the quality of the data. The CLEAN-maps (Fig. 1a and b) therefore include only components close to the core ($r \leq 1$ mas).

Owing to the sparseness of data and the uncertain errors at mm-wavelengths, the maps have a low dynamic range, and may exhibit spurious low-brightness features or may be affected by unrecognized sidelobes. Our discussion therefore will be mainly based on the results of model fits, which are more reliable than maps in the case of sparse uv-coverage. However, the representation of the basic structure of the source in the maps is consistent with the model fits. We obtained a quantitative description of the source structure (measurement of the flux densities and positions of the components visible in the maps) by fitting a number of elliptical Gaussian components to the data, using the model-fitting program of the Caltech-package. The detailed form of the visibility amplitudes and the closure phases[1] suggests that the data can be most simply represented by the models given in Table 1a and b. To ensure that the observed structural differences in the maps are not caused by differences in the uv-coverage at the two observing epochs, we investigated the influence on the visibilities of hypothetical components, hidden in gaps of the uv-coverage. In the region ($0.3 \leq r \leq 1.5$) mas, an extended elongated component with a flux density of $\sim$4 Jy may be hidden as low-level jet emission in the map of 1988.48. We can exclude that this emission is concentrated in one single bright, compact jet component, because of the observed form and amplitude scale of the visibilities. We adopt the commonly accepted scenario of the ejection of a jet component from an unresolved core and its subsequent motion along the jet.

A comparison between the total flux densities of 3C 273 during the VLBI experiments [$S_{43\,GHz}$(1988.48) = 28.6 Jy, $S_{43\,GHz}$(1989.19) = 24.7 Jy] and the measured flux densities in the

Table 1a. Model fit parameters (epoch 1988.48)

Comp.	Flux [Jy]	r [mas]	P.A. [°]	FWHM [mas]
1	18.4 ± 1.6	0	0	0.22 ± 0.06
2	2.8 ± 1.2	0.23 ± 0.06	246^{+30}_{-10}	0.23 ± 0.10
3	1.1 ± 0.4	2.8 ± 0.2	238 ± 5	0.19 ± 0.10

Table 1b. Model fit parameters (epoch 1989.19)

Comp.	Flux [Jy]	r [mas]	P.A. [°]	FWHM [mas]
1	13.4 ± 2.1	0	0	0.26 ± 0.06
2	1.8 ± 0.2	0.24 ± 0.06	271 ± 14	0.10 ± 0.04
3	1.4 ± 0.3	0.55 ± 0.10	253 ± 5	0.10 ± 0.04
4	5.3 ± 0.6	0.81 ± 0.02	245 ± 5	0.23 ± 0.06
5	0.9 ± 0.2	3.3 ± 0.2	223 ± 10	0.74 ± 0.20

[1] In contrast to previous 7mm VLBI experiments, which gave essentially little or no closure information for 3C 273, the measurement of these closure phases is mainly responsible for the fact that we were able to make maps and obtain well-defined model fits.

model fits, reveals that 80 to 90% of the total flux density is detected in our experiments. The missing flux density can be attributed to extended and resolved jet emission outside our field of view. An additional component not shown in the maps (Fig. 1a and b), at a distance from the core of $r = 2.8$ mas (1988.48), later $r = 3.3$ mas (1989.19), was found by model fitting. This component introduces a smooth curvature into the model closure phases of the data of 1988.48 and a much better fit to the B-T visibility amplitude in the data of 1989.19. The fact that for both epochs of observation this component is at a position expected from 10.7 GHz (Co87) and recent 22 GHz observations (Z90) is a strong argument for the reality of its existence. Table 1 shows the parameters of the Gaussian components from the model fits to the two epochs of observation (flux density, position, and the FWHM of the major axis). Errors are estimated formally (from the least square fit algorithm) and during the model-fitting procedure by using slightly different calibrated and edited datasets and starting models. From these two methods, the more conservative error estimate was taken. Figure 2 displays the fit of the models to the observed visibility amplitudes and closure phases.

4. Discussion

3C 273 underwent large, rapid infrared and optical flares between late February and early April 1988 (Courvoisier et al., 1988). During this period of enhanced acitivity, several events with amplitude increases of up to 40% on time scales as short as some days were observed. The flare with the highest amplitude occurred on March 10, 1988. We will use this data as the reference epoch of the outburst (1988.19).

At the same time the flux density at 230 GHz and 90 GHz increased rapidly (H. Steppe, priv. comm.). At 90 GHz an increase in flux density by a factor of at least ~ 1.5 ($S_{90\mathrm{GHz}} = 16.5$ Jy on February 12, 1988 and $S_{90\mathrm{GHz}} = 25$ Jy on March 8, 1988) in $\Delta t \leq 24$ d was measured (H. Steppe, priv. comm.). Such rapid flaring at this high frequency implies a brightness temperature

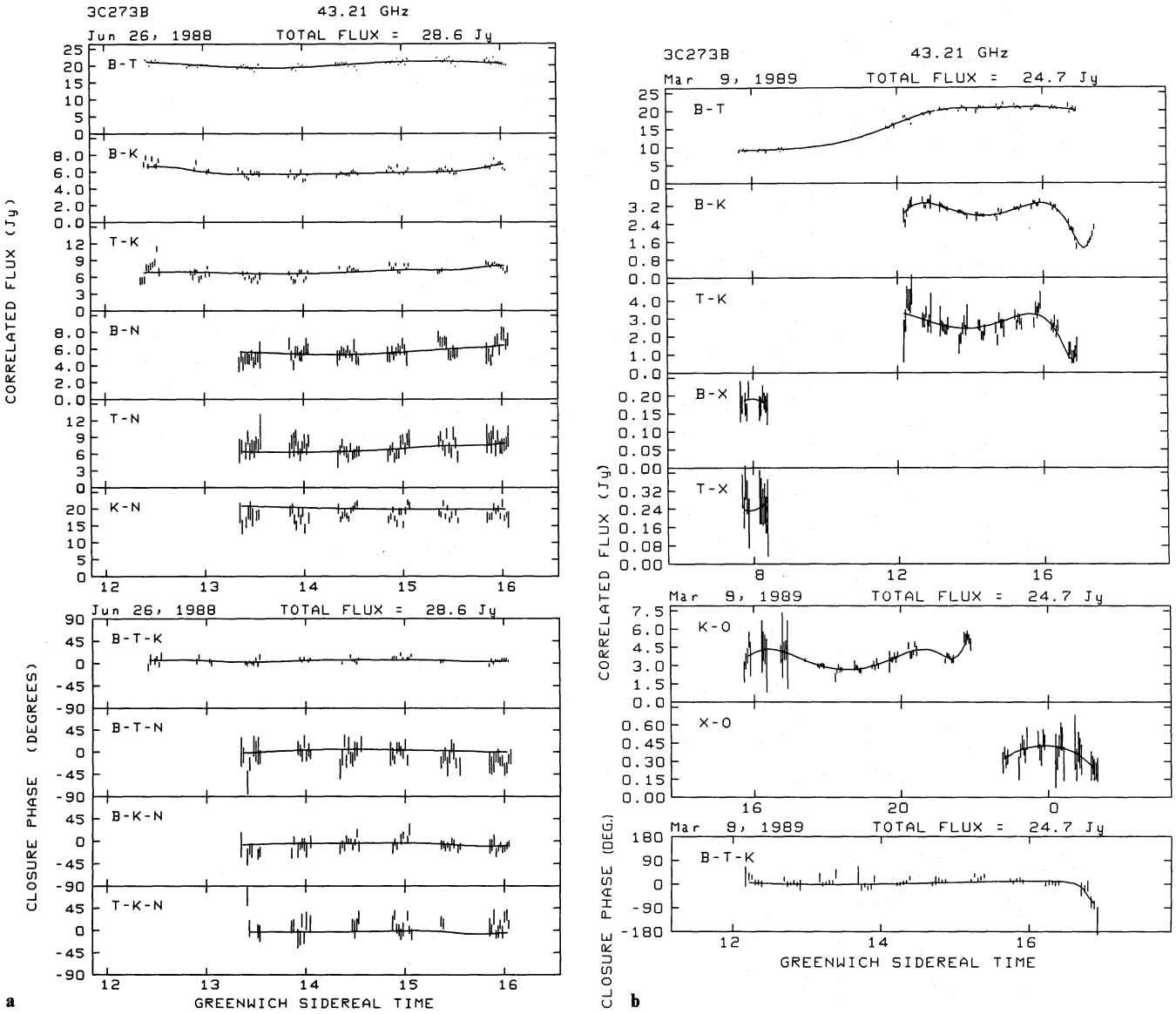

Fig. 2a and b. The visibility data, epoch 1988.48 and 1988.19. The measured visibility amplitudes and closure-phases with superimposed model fit

of $T_B^{90GHz} \geq 11 \cdot 10^{12}$ K, exceeding the inverse-Compton limit of $T_B = 10^{12}$ K (Kellermann and Pauliny-Toth, 1969) by at least an order of magnitude. This suggests relativistic Doppler boosting (e.g. Cohen and Unwin, 1984) in the variable core with a Doppler boosting factor $D \geq 2.2$. The spectral index $\alpha_{5/90GHz}$ ($S \propto \nu^{\alpha}$) of the total flux density of 3C 273 flattened dramatically from -1.1 (November 1987) to -0.15 (June 1988). At 43 GHz the total flux density reached a first maximum in June 1988 ($S_{43GHz} = 30.4$ Jy), and remained at this relatively high level at least until 1988.5 (Abraham, 1990, hereafter A90). At 37 GHz an increase in flux density from a minimum value of $S_{37GHz} = 16$ Jy in 1988.12 to a maximum of $S_{37GHz} = 35$ Jy in 1988.68 is clearly visible in the data of the Metsähovi flux density monitoring program (Valtaoja et al., 1988 and references therein; E. Valtaoja, priv. comm.). From this change in flux density we calculated a brightness temperature of $T_B^{37GHz} = 6 \cdot 10^{12}$ K, indicating that the brightness temperature decreases with decreasing frequency. A pronounced flux density maximum at 22 GHz, which peaked around 1988.92 (A90) may be interpreted as the time-delayed propagation of the flare through the spectrum. Thus the major characteristic of this outburst is a very rapid growth in amplitude over a wide frequency range (from the optical to the radio band). A comparable outburst with similar characteristics also occurred in 1983 (Robson et al., 1983; Robson et al., 1986) and has been interpreted as a shock wave passing through a relativistic jet (Marscher and Gear, 1985; Valtaoja et al., 1988).

The ejection of new superluminal components into a pre-existing jet is usually thought to be triggered by enhanced activity of the "central engine". It is observed for many AGN that the total flux density of the source and/or that of the compact VLBI core increases when a new VLBI component appears (e.g., BL Lac: Mutel and Phillips, 1987; 0836+71: Krichbaum et al., 1990a). However, observations of the structural variability of jet regions near the core soon after major flux density outbursts are still rare.

The time lag between the March 1988 IR/optical outburst and our detection of a new component at $r = 0.2$ mas is 108 d, indicating that the new component was ejected with an angular velocity $\mu = 0.8$ mas yr^{-1}, comparable to that of C 7 and C 8. Comparison of the maps in Fig. 1a and b shows clearly an increase in size of the envelope of emission near the core, also suggesting motion with a similar velocity. From the second epoch observation in 1989.19, the brightest secondary component, which accounts for the major features of the visibilities, is component 4 in Table 1b, at a radial distance $r = 0.8$ mas from the core. If we identify this component with the 0.2 mas component from 1988.48, the resulting angular motion of $\mu = (0.82 \pm 0.12)$ mas yr^{-1} and the extrapolated "zero spacing time" $t_0 = (1988.2 \pm 0.2)$ yr strongly suggest that a new component, which we now label C 9 (according to the established nomenclature), was generated during the preceding flare and is now moving outwards with apparent superluminal speed of $\beta_{app} = 5.5 \pm 0.8$ (see Table 2).

The map in Fig. 1b shows additional components in the region between C 9 and the core, at distances $r = 0.24$ mas and $r = 0.55$ mas (components 2 and 3 in Table 1b). An identification of one of these components with the 0.2 mas component of 1988.48 (component 2 in Table 1a) seems not plausible, since the resulting apparent velocities would be much lower than expected for this source and the extrapolated times of zero separation cannot be attributed to pronounced flux density changes.

Structural changes close to the core ($r \leq 0.3$ mas) of 3C 273 were also detected in previous 43 GHz snapshot experiments from 1985, 1986, and 1987 (Marcaide et al., 1985; Dhawan, 1987; Bartel et al., 1988). From these data we find that an increase of the correlated flux density on long baselines was accompanied by a general flattening of the total source spectrum. However, because of the limited data available and the probably complex source structure no models or maps could be made for these early observations.

Independent evidence for emission close to the core at position angles similar to those we observed [P.A. $\simeq (240 - 260)°$] is also provided by recent 100 GHz VLBI measurements (Epoch 1988.21) of 3C 273 (Bååth, 1990). These observations show at least two secondary components close to the brightest feature (possibly the core) at $r \simeq 0.1$ mas and $r \simeq 0.25$ mas. Thus, from independent and closely spaced VLBI observations at 43 and 100 GHz, a core-jet structure oriented in east-west direction is confirmed consistently. The above numbers also suggest a possible, though speculative identification of the component at $r = 0.1$ mas with C 9.

As mentioned above, the brightness temperature of the source, derived from its variability at 90 GHz, exceeds the inverse Compton limit by a factor of ≥ 11. Assuming that the jet components move at an inclination angle i_{max} to the observer's line of sight which maximizes the observed apparent superluminal velocity β_{app}, a minimum Lorentz factor $\gamma_{min} = 5.5$ and a Doppler factor of $D = \gamma^{-1}(1 - \beta \cos i_{max})^{-1} \simeq 11$ is derived. This is consistent with the lower limit of D calculated from the flux density variability. Using the parameters of the core derived from the model fit (see Table 1a, component 1), a brightness temperature of at least $2.5 \cdot 10^{11}$ K is calculated for the epoch nearest to the outburst, decreasing to $1.3 \cdot 10^{11}$ K in 1989.19, indicating now a decreasing activity of the "central engine" of 3C 273.

Table 2. Position changes of the inner jet components

Comp.	t_0 [yr][a]	μ [mas yr^{-1}]	β_{app}	d(P.A.)/dr [deg mas^{-1}]	Comment
C 4	1976.0 ± 0.6	0.99 ± 0.24	6.6 ± 1.6	-0.8 ± 0.5	U85, Co87
C 5	1978.6 ± 0.2	1.20 ± 0.03	8.0 ± 0.2	-1.5 ± 0.6	U85, Co87
C 7	1982.0 ± 0.2	0.59 ± 0.05	4.0 ± 0.3	2.7 ± 0.9[b]	Co87, Z90, A90
C 8	1984.6 ± 0.2	0.76 ± 0.05	5.1 ± 0.3	1.8 ± 1.3	Z90, A90, this paper
C 9	1988.2 ± 0.2	0.82 ± 0.12	5.5 ± 0.8	-19 ± 36	This paper

[a] Zero spacing epoch extrapolated from a linear regression analysis.
[b] Using components C 7a and C 7b.

On the assumption that the core emission is dominated by synchrotron radiation from a self-absorbed homogeneous sphere (with turnover frequency $\nu_{max} \geq 43$ GHz), a magnetic field $B \geq (2-5)\cdot 10^{-2} D$ G (with Doppler factor $D \simeq 10$) is derived. From the optical variability, Courvoisier et al. (1989) derive a magnetic field $B = 0.7$ G in the core, assuming synchrotron cooling close to the cut-off frequency. Thus both results for the field strength are of the same order of magnitude for the adopted value of the Doppler factor. A very similar magnetic field strength of $B \simeq 0.15$–1.0 G has also been derived by Marscher and Gear, 1985 for the IR/mm-flare of 3C 273 in 1983. This suggests that the magnetic field in the proximity of the core is relatively high and may be dynamically important, i.e., could be responsible for the observed curved trajectories in the jet.

The component at $r = 2.8$ mas (component 3 in Table 1a) and at $r = 3.3$ mas (component 5 in Table 1b) may be identified with component C 8 in the 10.7 GHz maps of Co87. This identification is supported by the 22 GHz observations (Z90). From those data, the distance of C 8 from the core can be linearly extrapolated to our observing epochs. The extrapolated positions agree very well with those measured by us. In Fig. 3 we plot the separation of the components C 5, C 7, C 8, and C 9 from the core versus time (Unwin et al., 1985, hereafter U85; Charlot et al., 1987; Co87, Z90, and Zensus, priv. comm.), together with the new 43 GHz data for C 8 and C 9 (enlarged symbols). To each component we fitted a straight line. Table 2 summarizes the resulting angular motion μ [mas yr^{-1}] (Table 2, col. 3), apparent velocity $\beta_{app} = v_{app}/c$ (Table 2, col. 4), and the extrapolated "zero spacing time" t_0 (the time for which $r = 0$, Table 2, col. 2). Formal errors are given from the regression analysis. From these data, the observed angular velocity μ of the components ranges between 0.6 and 1.2 mas yr^{-1}, with no evidence for acceleration or deceleration for each component. It is obvious that different components exhibit different velocities.

For 3C 273 a correlation between flux density outbursts in the high frequency radio regime and the appearance of new superluminal jet components is suggested by our observations and the published observational data. The extrapolated time of origin for each of the jet components C 4 to C 9 (see column 2 in Table 2) coincides well with the *beginning* of increases in flux density, which are visible in the radio lightcurves of 3C 273 (43 GHz and 22 GHz: Botti and Abraham, 1988; 37 GHz and 22 GHz: Salonen et al., 1987). The typical amplitudes of these outbursts are $\Delta S_{22\,GHz} = 8 - 15$ Jy. Less well pronounced flux density increases can also be seen in the data at lower frequencies (e.g. at 10.7 GHz: Aller et al., 1985; Haddock et al., 1987). The time lag between the beginning of an outburst (defined as the minimum of flux density closest to a subsequent pronounced flux density maximum) and the subsequent maximum in flux density is typically $\Delta t_m = (0.4 - 0.8)$ yr (at 43 GHz and 22 GHz). Adopting a typical angular velocity of $\mu \simeq 0.8$ mas yr^{-1} for a newly expelled jet component, the distance at which the total flux density of the source becomes brightest is of order $r_{max} = \mu \Delta t_m \simeq (0.3 - 0.6)$ mas. This is in quantitative agreement with the evolution of C 9. The brightness temperature of C 9 nearly doubled while this component moved from $r = 0.2$ mas to $r = 0.8$ mas. Even allowing for possible calibration errors, this increase remains significant. From observations at lower frequencies which are sensitive to somewhat larger core distances ($r \geq r_{max}$), Co87 and Z90 report that secondary components decay in brightness as they move out. Thus it seems reasonable to assume that in 3C 273 after a flux density outburst the ejected component is at first self-absorbed and becomes optically thin in a later stage of evolution. In the region $r \leq r_{max}$ the opacity probably decreases with time and therefore with r, causing the observed brightening of C 9. On the basis of the 22 GHz data of earlier components (Co87, Z90) a decay in flux density could be expected for $r \geq r_{max}$, but further VLBI observations are required to follow the spectral evolution of C 9.

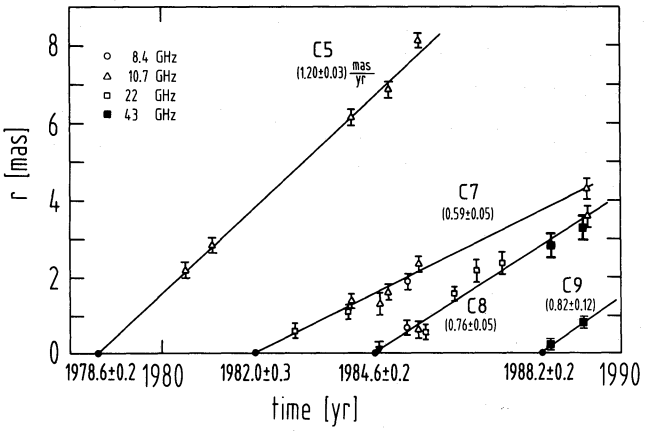

Fig. 3. The expansion diagram for the jet components. Separation versus time is plotted for components C 5 through C 9. Symbols denote different frequencies. *Open circles* 8.4 GHz (Charlot et al., 1987), *open triangles* 10.7 GHz (Co87; Zensus, priv. comm.), *open squares* 22 GHz (Z90), *filled squares* 43 GHz (this paper). From regression analysis, fit lines are superimposed. The separation rate is shown for each component. Extrapolated "zero spacing epochs" are indicated by *filled circles* on the time axis

In the case of C 9 a correlation between t_0 and the time of an IR/optical flare is highly probable; however, due to more measurements available now for C 7, we cannot confirm the correlation of a similar IR/optical flare in early 1983 (Robson et al., 1983; Robson et al., 1986) with this component. Possible explanations could be that either this flare did not produce any observed VLBI component, or that such a component was short-lived or merged with another component. Co87 find an additional component C 7b next to C 7 at 10.7 GHz. The extrapolated zero spacing time for C 7b from only 3 epochs of observation is (1982.1 ± 1.1) yr, marginally coincident with the epoch of the 1983 flare.

In a simple model, flux density outbursts indicate rapid changes in the density distribution of the radiating synchrotron electrons, which could result in a relativistic shock ("blast-") wave (Blandford and McKee, 1977; Begelman et al., 1984), propagating into an already existing relativistic jet. Following such a primary shock, which here may be attributed to the brightest jet component (C 9), additional weaker shocks are not unexpected in the post-shocked regions (Norman et al., 1983), especially if the central energy-supplying machine remains active on a reduced level. Such continuing activity is suggested by the relatively high level of the total flux density of 3C 273 at 43 GHz between 1988 and 1989 (A90). Thus the radiation from the fainter intermediate jet components (components 2 and 3 in Table 1b) could be assigned to this activity. We further note that the optical/infrared outburst was composed out of several flares, which also could introduce a more complex shock pattern, leading to the observed brightness distribution. Further flux density monitoring combined with high frequency VLBI monitoring is necessary to obtain further constraints on the model.

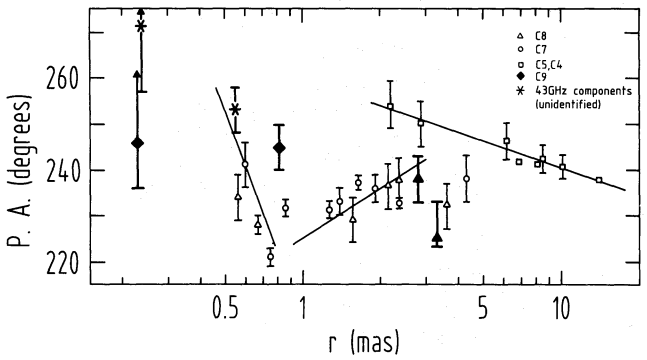

Fig. 4. The bending of the inner VLBI-jet. The location of the centroids of the jet components of 3C 273 in a plot of position angle versus core distance. Symbols denote different jet components; *open squares* are for C 4 and C 5, *open circles* for C 7, *triangles* for C 8 (*filled triangles* from the 43 GHz experiments), *filled diamonds* for C 9, *asterisks* for two new, not yet identified 43 GHz components. Data not from 43 GHz observations are from U85; Co87, Z90 and Zensus, priv. comm. The 43 GHz data are marked by enlarged filled symbols

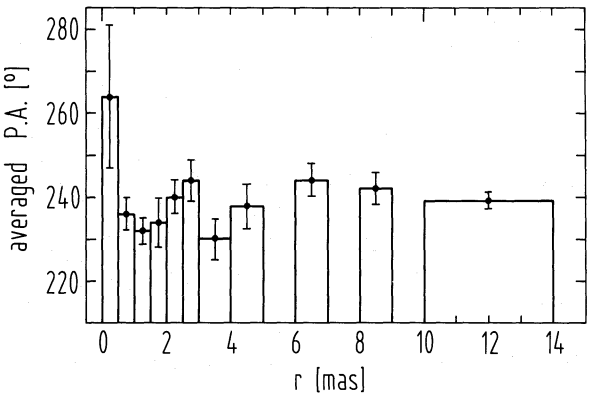

Fig. 5. The mean ridgeline of the jet. The binned and averaged position angle (see text) of the jet components in Fig. 4 plotted versus the distance from the core

The jet of 3C 273 is well pronounced, partially sinusoidally oscillating and extends out to at least 20″ (Z88; Davis et al., 1985). To measure the ridge line of the VLBI jet, we combined all available data from the literature with our observations. Following Co87, we display in Fig. 4 the position angle P.A. of the jet components with respect to the core versus their distance r from the core. A linear regression analysis yields the formal rate of change d(P.A.)/dr, a measure of the curvature of the trajectory of each component. Table 2, column 5 summarizes this result. From Table 2 and Fig. 4 the components C 4 and C 5 seem to move on a common curved trajectory, with P.A. decreasing with increasing distance. In contrast, the P.A. increases with distance for the components C 7 and C 8 ($1\,\text{mas} \leq r \leq 4\,\text{mas}$). For these two components, the data are consistent with a common curved trajectory, which may however be different from that of C 4 and C 5. The large errors on the P.A. of C 9 do not allow us to estimate its path accurately. However, as is obvious from the maps, the jet of 3C 273 bends from P.A. $\simeq 260°$ at $r = 0.2$ mas to P.A. $= 245°$ at $r = 0.8$ mas. This is indicated by straight lines added to Fig. 4. The P.A. may decrease with increasing r within $(0.2 \leq r \leq 1)$ mas. More data are needed to follow the path of C 9 and those of the additional components at $r = 0.24$ mas and $r = 0.55$ mas (Table 1b). In order to display the bending in 3C 273 more clearly, we divided Fig. 4 into bins of width Δr and averaged the values of the P.A. for all components within each bin. The resulting histogram is shown in Fig. 5. Since only few data are available for $r \leq 0.8$ mas, the jet bending in this region must still be regarded with some care. The occurrence of bending along the entire jet is not unexpected since the source also displays pronounced bends on larger scales (see e.g. the 5 GHz map in Z88). Figure 5 then measures the ridge line of the inner jet, which appears as a quasi-sinusoidally varying track.

Three-dimensionally (e.g. helically) bent jets should display differential Doppler boosting [that means a Doppler factor varying as a function of the local inclination angle i to the observers line of sight of the jet components, $D(i) = \gamma^{-1}(1 - \beta \cos i)^{-1}$] and therefore velocity changes $\beta_{\text{app}}(i)$ of components along the jet. In Table 2 the apparent velocities β_{app} of components C 9 to C 4 are summarized. Although the errors are large a systematic variation of β_{app} seems obvious. The velocities of C 9 to C 7 decrease from 5.5c to 4.0c. The velocity of C 5 is quite high (8.0c) whereas the velocities of the older components C 4 and C 3 again are lower (C 4: 6.6c, C 3: 5.3c; U 85). Recent observations indicate that for component C 2 the velocity is higher than for C 4 and C 3 ($\beta_{\text{app}} = 6.7 - 8.7$, Z88). Thus there is some evidence for a periodic or at least quasi-periodic variation of β_{app} within the VLBI components of 3C 273. An oscillating jet axis with alternating changes of the mean jet inclination $i \pm \Delta i$ of $\Delta i \simeq$ a few degrees may explain the apparent variation of β_{app}. From Fig. 4, the curvature in the motion of C 7 and C 8 is d(P.A.)/dr $\simeq +(2-3)°\,\text{mas}^{-1}$ while that of C 5, C 4, and C 3 is d(P.A.)/dr $\simeq -(1-2)°\,\text{mas}^{-1}$ (see Table 2, Co87, Z88, and references therein). In regions $r \leq 0.8$ mas the curvature is probably negative. These changes of sign of d(P.A.)/dr with r, in combination with the possible velocity gradients along the jet for the different components, suggest motion along a helical path.

Motion along curved trajectories is so far established only for 3C 345 (Biretta et al., 1986). 7mm-VLBI observations in combination with VLBI observations at lower frequencies (especially at 22 GHz) suggest, that strongly bent jets in regions close to the core are a common phenomenon and appear not only in 3C 345 (Krichbaum, 1990b; Zensus et al., 1990b) and 3C 273, but also in 3C 84 (Krichbaum, 1990b and 1900c; Readhead et al., 1990; Marr et al., 1990) and 1803+78 (Krichbaum, 1990b and 1990c).

The oscillations and bends of jets may be interpreted as due to Kelvin-Helmholtz instabilities (e.g., Hardee, 1987), by precession of the central source of energy (e.g., Roos, 1988) or by models involving magnetized jets (Camenzind, 1986; Königl and Choudhuri, 1985). Motion along curved trajectories is not expected for precessing jets, where components should move ballistically. In relativistic jets, hydrodynamical instabilities are expected and may be responsible for apparently curved paths. To allow for component motion along a fixed and curved path, the lifetime of the instability must be longer than the interval between the appearance of new jet components, so that adjacent jet components encounter the same physical conditions and are deflected in a similar manner. Instabilities tend to disrupt a jet. An instability in regions very close to the core must be so weak that the jet is not disrupted or recollimation must occur. Otherwise, long and pronounced jets (as is the case in 3C 273) would not be observable.

On the other hand, motion along fixed curved paths may be interpreted within magneto-hydrodynamical jet models, in which the magnetic field determines or influences the jet propagation. Such a scenario is supported by polarization VLBI measurements (Roberts and Wardle, 1987), and by the relatively large magnetic field strengths deduced for the core region of 3C 273. Assuming for example a helical magnetic field geometry, the observed strong bending of the jet and the motion of the VLBI components along fixed trajectories at parsec and sub-parsec scales may reflect the field geometry. The observed sinusoidal bending, which is larger at smaller distances from the core, may then be indicative of a magnetic field structure, twisted by rotation of its generator (Camenzind, 1986; Camenzind, 1989).

5. Summary

The first 43 GHz images of 3C 273 are presented. The source exhibits rapid evolution towards a complex jet structure. A new superluminal jet component (which we label C 9) is detected in two epochs of VLBI observations at 43 GHz. This component has been attributed to the large IR/optical outburst in early 1988 and the associated increase of the flux density in the radio band, which was observed in early 1988. Additional jet components, closer to the core than C 9, indicate either a continuing enhanced activity of the core, or require more complicated jet physics. The investigation of the expansion graphs (Fig. 3) of components C 4 through C 9 leads to a correlation between "zero spacing times" with the *beginning* of total flux density increases at mm-wavelengths.

The position of the new component C 9 relative to the core differs from the direction to the outer jet. The latter displays transverse oscillations at lower frequencies (Z88). Taking into account the new 43 GHz data, a possible quasi-sinusoidal bending (bends followed by reverse bends) of the jet within ($0.2 \leq r \leq 14$) mas is indicated (see Figs. 4 and 5). A possible systematic variation of the apparent velocities of the jet components C 2 to C 9 supports the hypothesis of an oscillating jet axis.

The identification of C 8 at 10.7 GHz (Co87; Zensus, priv. comm.), 22 GHz (Z90) and 43 GHz leads to apparent superluminal motion along a curved trajectory, similar to that of the earlier component C 7. Superluminal motion along curved trajectories in a bent jet is also seen in 3C 345 (Biretta et al., 1986; Zensus et al., 1990b) and is still neither well understood nor established for many sources. Further monitoring of 3C 273 at mm-wavelengths will clarify how the components seen at 43 GHz move outwards and whether they follow the path defined by previously ejected (older) jet components.

Acknowledgements. We are grateful to the technical staff of the observatories participating in 7 mm-VLBI, and to all individuals who helped in many ways to make these technically and logistically difficult experiments possible. At the MPIfR, special thanks are due to Dr. W. Alef for his tireless help and advice with the data reduction, to Mr. H. Blaschke and Mr. U. Stursberg for their efforts at the Mark III correlator, to Dr. W. Altenhoff for his help with the single-dish calibration, and to Dr. R. Schwartz and W. Zinz for their support. At Owens Valleys, this work would be impossible without the continuing enthusiastic work of Dr. H. Hardebeck and Dr. M. Hodges.

The National Radio Astronomy Observatory is operated by Associated Universities, Inc., under cooperative agreement with the National Science Foundation (NSF). VLBI research at Owens Valley is supported by the NSF under Grant AST 88-14554 AJR. The work at Haystack Observatory is also, in part, supported by the NSF.

References

Abraham, Z.; 1990, in: *Parsec-scale Radio Jets*, eds. J.A. Zensus and T.J. Pearson, Proceedings of a NRAO-workshop held in Socorro October 1989, Cambridge University Press, Cambridge (in press) (A90)

Alef, W., Porcas, R.W.: 1986, *Astron. Astrophys.* **168**, 365

Alef, W.: 1988a, in *Very Long Baseline Interferometry Techniques and Applications*, Proceedings of the NATO Advanced Study Institute on VLBI, eds. M. Felli and R.E. Spencer, p. 97

Alef, W., Götz, M.M.A., Preuss, E., Kellermann, K.I.: 1988b, *Astron. Astrophys.* **192**, 53

Aller, H.D., Aller, M.F., Latimer, G.E., Hodge, P.E.: 1985, *Astrophys. J. Suppl.* **59**, 513

Begelman, M.C., Blandford, R.D., Rees, M.J.: 1984, *Rev. Modern Phys.* **56**, 255

Botti, L.C., Abraham, Z.: 1988, *Astron. J.* **96**, 465

Bååth, L.: 1990, in *Parsec-scale Radio Jets*, eds. J.A. Zensus and T.J. Pearson, Cambridge University Press, Cambridge (in press)

Bartel, N., Dhawan, V., Krichbaum, T., Graham, D., Pauliny-Toth, I.I.K., Rogers, A.E.E., Rönnäng, B.O., Spencer, J.H., Hirabayashi, H., Inoue, M., Lawrence, C.R., Shapiro, I.I., Burke, B.F., Marcaide, J.M., Johnston, K.J., Booth, R.S., Witzel, A., Morimoto, M., Readhead, A.C.S.: 1988, *Nature* **334**, 131

Biretta, J.A., Cohen, M.J., Hardebeck, H.E., Kaufmann, P., Abraham, Z., Perfetto, A.A., Scalise, E., Jr., Schaal, R.E.: 1985, *Astrophys. J.* **292**, L5

Biretta, J.A., Moore, R.L., Cohen, M.H.: 1986, *Astrophys. J.* **308**, 93

Camenzind, M.: 1986, *Astron. Astrophys.* **156**, 137

Camenzind, M,: 1989, in *Accretion Disks and Magnetic Fields in Astrophysics*, ed. G. Belvedere, Kluwer, Dordrecht, p. 129

Charlot, P., Lestrade, J.-F., Boucher, C.: 1987, in *IAU Symp.* **129**, eds. M. Reid and J. Moran, Kluwer, Dordrecht, p. 33

Clark, B.G.: 1973, *Proc. I.E.E.E.* **61**, 1242

Cohen, M.H., Unwin, S.C.: 1984, *IAU Symp.* **110**, p. 95

Cohen, M.H., Zensus, J.A., Biretta, J.A., Comoretto, G., Kaufmann, P., Abraham Z.: 1987, *Astrophys. J.* **315**, L89 (Co87)

Courvoisier, T.J.L., Robson, E.I., Blecha, A., Bouchet, P., Hughes, D.H., Krisciunas, K., Schwarz, H.E.: 1988, *Nature* **335**, 330

Davies, R.J., Muxlow, T.W.B., Conway, R.G.: 1985, *Nature* **318**, 343

Dhawan, V.: 1987, Ph.D. thesis, Massachusetts Institute of Technology, Cambridge

Haddock, T.F., Aller, H.D., Aller, M.F.: 1987, *Astron. J.* **93**, 1356

Hardee, P.E.: 1987, *Astrophys. J.* **318**, 78

Kellermann, K.I., Pauliny-Toth, I.I.K.: 1969, *Astrophys. J.* **155**, L71

Königl, A., Choudhuri, A.R.: 1985, *Astrophys. J.* **289**, 173

Krichbaum, T.P., Hummel. C.A., Quirrenbach, A., Schalinski, C.J., Witzel, A., Johnston, K.J., Muxlow, T.W.B., Qian, S.J.: 1990a, *Astron. Astrophys.* **230**, 271

Krichbaum, T.P.: 1990b Ph.D. thesis, University of Bonn
Krichbaum, T.P.: 1990c, in *Parsec-scale Radio Jets*, eds. J.A. Zensus and T.J. Pearson, Cambridge University Press, Cambridge (in press)
Norman, M.L., Winkler, K.H.A., Smarr, L.: 1983, in *Astrophysical Jets*, eds. A. Ferrari and A.G. Pacholczyk, Reidel, Dordrecht, p. 227
Marcaide, J.M., Pauliny-Toth, I.I.K., Graham, D.A., Rönnäng, B., Booth, R.S., Bartel, N., Shapiro, I.I., Rogers, A.E.E., Dhawan, V., Burke, B.F., Johnston, K.J., Spencer, J.H.: 1985, in *Proc. IRAM-ESO-Onsala Workshop on (Sub-) Millimeter Astronomy*, eds. Shaver, P.A. and Kjär, K., p. 157
Marr, J.M., Backer, D.C., Wright, M.C.H.: 1990, in *Parsec-scale Radio Jets*, eds. J.A. Zensus and T.J. Pearson, Cambridge University Press, Cambridge (in press)
Marscher, A.P., Gear, W.K.: 1985, *Astrophys. J.* **298**, 114
Mutel, R.L., Phillips, R.B.: 1987, in: *Superluminal Radio Sources*, eds. J.A. Zensus and T.J. Pearson, Cambridge University Press, Cambridge, p. 60
Readhead, A.C.S., Venturi, T., Marr, J.M., Backer, D.C.: 1990, in *Parsec-scale Radio Jets*, eds. J.A. Zensus and T.J. Pearson, Cambridge University Press, Cambridge (in press)
Roberts, D.J., Wardle, F.F.C.: 1987, in *Superluminal Radio Sources*, ed. J.A. Zensus and T.J. Pearson, Cambridge University Press, Cambridge, p. 193
Robson, E.I., Gear, W.K., Clegg, P.E., Ade, P.A.R., Smith, M.G., Griffin, M.J., Nolt, I.G., Radostitz, J.V., Howard, R.J.: 1983, *Nature* **305**, 194
Robson, E.I., Gear, W.K., Brown, L.M.J., Courvoisier, T.J.L., Smith, M.G., Griffin, M.J., Blech, A.: 1986, *Nature* **323**, 134
Rogers, A.E.E., Capallo, R.J., Hinteregger, H.F., Levine, J.I., Nesman, E.F., Webber, J.C., Whitney, A.R., Clark, T.A., Ma, C., Ryan, J., Corey, B.E., Counselman, C.C., Herring, T.A., Shapiro, I.I., Knight, C.A., Shaffer, D.B., Vandenberg, N.R., Lacasse, R., Mauzy, R., Rayhrer, B., Shupler, B.R., Pigg, J.C.: 1983, *Science* **219**, 51
Roos, N.: 1988, *Astrophys. J.* **334**, 95
Salonen, E., Teräsranta, H., Urpo, S., Tiuri, M., Moiseev, I.G., Nesterov, N.S., Valtaoja, E., Haarala, S., Lehto, H., Valtaoja, L., Teerikorpi, P., Valtonen, M.: 1987, *Astron. Astrophys. Suppl.* **70**, 409
Schalinski, C.J., Witzel, A., Krichbaum, T.P., Hummel, C.A., Biermann, P.L., Johnston, K.J., Simon, R.S.: 1987, in *IAU Symp.* **129**, eds. M.J. Reid and J.M. Moran, Kluwer, Dordrecht, p. 71
Unwin, S.C., Cohen, M.H., Biretta, J.A., Pearson, T.J., Seielstad, G.A., Walker, R.C., Simon, R.S., Linfield, R.P.: 1985, *Astrophys. J.* **289**, 109 (U85)
Valtaoja, E., Haarala, S., Letho, H., Valtaoja, L., Valtonen, M., Moiseev, I.G., Nesterov, N.S., Salonen, E., Teräsranta, H., Urpo, S., Tiuri, M., 1988, *Astrophys. J.* **203**, 1
Witzel, A., Schalinski, C.J., Johnston, K.J., Biermann, P.L., Krichbaum, T.P., Hummel, C.A., Eckart, A.: 1988, *Astron. Astrophys.* **206**, 245
Zensus, J.A., Bååth, L.B., Cohen, M.H., Nicolson, G.D.: 1988, *Nature* **334**, 410 (Z88)
Zensus, J.A., Unwin, S.C., Cohen, M.H., Biretta, J.A.: 1990a *Astrophys. J.* (submitted) (Z90)
Zensus, J.A., Krichbaum, T.P., Lawrence, C.R., Readhead, A.C.S., Witzel, A., Graham, D.A., Pauliny-Toth, I.I.K., Rogers, A.E.E., Hirabayashi, H., Inoue, M., Morimoto, M., Booth, R., Kus, A., Rönnäng, B.O., Johnston, K.J., Spencer, J., Dhawan, V., Bartel, N., Marcaide, J.M., Burke, B.F.: 1990b (in preparation)